

REFINEMENT OF ADTI-WP2 STANDARD WEATHERING PROCEDURES, AND EVALUATION OF PARTICLE SIZE AND SURFACE AREA EFFECTS UPON LEACHING RATES: PART 2: PRACTICAL AND THEORETICAL ASPECTS OF LEACHING KINETICS¹

K.B.C. Brady,² W.B. White, R.J. Hornberger, B.E. Scheetz, and C.M. Loop

Abstract: Most previous coal mine drainage leaching studies have not investigated the effect of surface area, effects of elevated P_{CO_2} , which are typical of mine spoil, and solubility constraints on water chemistry. The leaching column and humidity cell tests were designed to evaluate the importance of these parameters. Surface area was examined on three rock types before and after leaching: the Brush Creek shale; a well-indurated calcareous sandstone; and a coal refuse. The surface area, as measured by BET, for the shale was an order of magnitude greater than the other rock types. Surface area after leaching decreased slightly for the shale, and by half for the refuse. The sandstone area remained the same. Plots of sulfate concentration through time closely resemble those expected for diffusion-controlled kinetics. Plots of alkalinity through time are characteristic of a material that dissolves quickly at first and then approaches or reaches saturation. Saturation with respect to calcite was confirmed by equilibrium calculations. The water in the leaching columns was undersaturated with respect to gypsum, indicating that sulfate was a conservative parameter and could be used to measure pyrite oxidation rates. The target 10% CO_2 was achieved in the column tests, but not achieved in the humidity cell tests. At the end of 12 to 14 weeks, between 1.5 and 2% of the calcite and between 4 and 6% of the sulfur in the rock had been removed by weathering. Predictions, based on power function equations, indicate that the Brush Creek shale sample would remain alkaline even if weathered for years. Comparisons between leaching chemistry and field data for the Brush Creek shale and the coal refuse sample showed similar water chemistry.

Additional Key Words: weathering tests, acid mine drainage, surface area effects, weathering rates, carbonate dissolution, pyrite oxidation.

¹Paper was presented at the 2004 National Meeting of the American Society of Mining and Reclamation and The 25th West Virginia Surface Mine Drainage Task Force, April 18-24, 2004. Published by ASMR, 3134 Montavesta Rd., Lexington, KY 40502.

²K.B.C. Brady is a Geologist, Pennsylvania Department of Environmental Protection (PA DEP), Harrisburg, PA 17105. W.B. White is Professor Emeritus Geochemistry, Materials Research Institute (MRI), Pennsylvania State University (PSU), University Park, PA 16802 R.J. Hornberger is a Geologist, PA DEP, Pottsville, PA 17901 B.E. Scheetz is Senior Scientist and Professor of Materials, MRI, PSU, University Park, PA 16802. C.M. Loop is a Postdoctoral Scholar, MRI, PSU, University Park, PA 16802
Proceedings America Society of Mining and Reclamation, 2004 pp 174-200
DOI:10.21000/JASMR04010174

<https://doi.org/10.21000/JASMR04010174>

Introduction

In the comprehensive literature review completed by Hornberger and Brady (1998), the authors detailed in excess of 90 leaching protocols that had been developed over the years. Most were developed to identify the potential for overburden rock units to produce acid mine drainage and to scale the magnitude of the potential effects. This study examines several aspects of leaching that have not been adequately addressed in the mine drainage literature. Areas addressed in this study include surface area effects, the effects of CO₂ on carbonate weathering, and solubility controls on leaching concentrations. Particle size was controlled in this study by using a preset proportion of sieve sizes, as described in Part 1 of this report (Hornberger et al., 2004). Surface area was determined using the Brunauer, Emmet and Teller (BET) method described below. The data for the study described below are based on column and humidity cell experiments as described in Part 1.

Studies show that carbon dioxide levels in mine spoil are frequently orders of magnitude greater than under atmospheric conditions (Cravotta et al., 1994; Lusardi and Erickson, 1985). Calcite is more soluble at high Pco₂ than under atmospheric conditions (White, 1988). Thus, the leaching procedure was designed to simulate mine spoil pore gas composition by using an elevated Pco₂. Calcite saturation limits the concentration of calcite products that can be dissolved in a solution. All other things being equal, the higher the Pco₂, the more calcite can be dissolved and the greater the concentration of calcite dissolution products in solution.

Pyrite oxidation is related to oxygen availability, which throughout the tests was more than adequate to allow oxidation. Pyrite oxidation is much less limited by solubility constraints than is calcite. With the addition of 10% CO₂ to atmospheric air, the oxygen concentration would be ~18.8% and well above levels needed for pyrite oxidation (Hammack and Watzlaf, 1990). Gypsum solubility was determined in this study because of the Brush Creek Shale's relative abundance of Ca and potential for producing SO₄. If gypsum was over-saturated it could limit the amount of sulfate in solution, by allowing gypsum precipitation, and affect the calculations of pyrite oxidation rates. Knowing that sulfur in solution behaved conservatively allowed its use as a measure of pyrite oxidation rates.

Concerns with Surface Area

One of the shortcomings of previous leaching studies has been not considering the effects of surface area and particle size. This factor was extensively studied in the decade from the mid-1970's through the mid-1980's by scientists who were investigating the stability of materials used for the sequestration of nuclear waste (e.g. Ethridge et al., 1979; Hench et al., 1980; Buckwalter et al., 1982; Oversby, 1982; Pederson et al., 1982;). It was recognized by this group of researchers that the particle size of the leached materials and the volume of fluid that was available for the leaching process had a significant impact on the experimental results. Fig. 1 demonstrates this dependence. Shown is the release of silica from a nuclear waste form as a function of time with specific control of the surface area to volume ratio.

What is important in this figure is that by specifically including the surface area/volume parameter, leaching rates varying over 3 orders of magnitude can be scaled onto the same plot. Surface area must also be taken into account in coal overburden leaching experiments. Otherwise the cross-laboratory experiments, although individually correct, cannot be compared, cannot be compared with other results in the literature, and cannot be used to extract quantitative rate constants. The observed leach rates would be an accurate result of the individual experiment, but meaningless as a fundamental property of the material itself.

In most of the protocols detailed in Hornberger and Brady (1998), a prescription is presented on the geometry, frequency of sample collection, and amount of material to be leached, but no detailed accounting was made of these parameters nor were the data utilized in any analytical sense. By contrast, leach protocols outlined in this paper established a procedure under which the crushed rock or coal refuse to be leached was sieved, and the contents of the columns constructed from specified sieve fractions to yield a common particle size distribution across laboratories. Further, the surface area of the rock was determined both before and after the leaching cycle was completed. With these data, an effective area of materials that were leached could be calculated for each column removing the necessity that each laboratory identically pack each column, a nearly impossible requirement for any protocol.

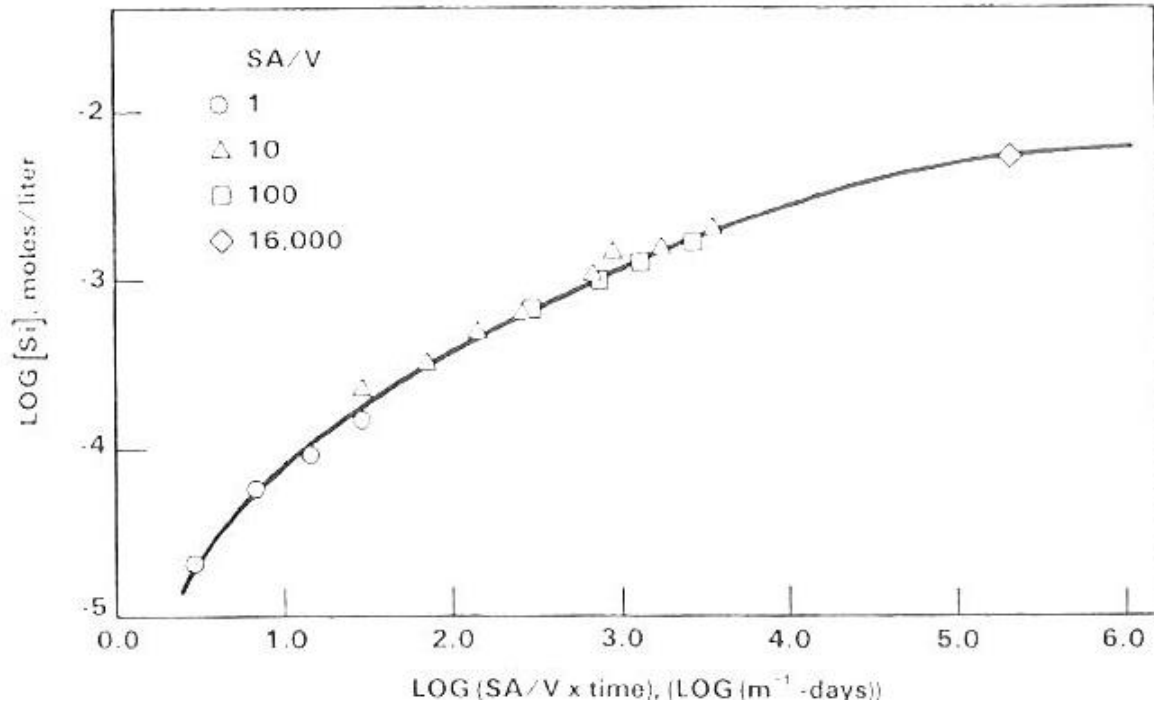


Figure 1. Log [Si] vs Log SA/V x t for a glassy nuclear waste form (after Pederson et al., 1983).

Measurement of Surface Area.

For this study, the surface area of each fraction of sieved starting material was determined by BET (Brunauer et al., 1938; Yates, 1992) instrumentation using N₂ gas bulk adsorption. This method is a routine analytical approach to measure the accessible surface of the rock to gas molecules. In the analytical procedure the rock specimen is heated to degas the surface in a heated vacuum cell. This step is followed by the introduction of gas back into the cell. The final step is to drive off the newly adsorbed gas and measure the quantity released. Knowing the volume of the gas and the molecular diameter of the particular gas, an accurate surface area can be calculated. Gases other than N₂ can be used but they would possess a different molecular size and thus a different quantity of gas would be needed to cover the same surface area. Therefore, it becomes necessary to specify the gas used in the measurement. Additional discussion of surface area measurements and their relationships to porosity and reaction kinetics is given by Brantley and Mellott (2002).

Surface areas were measured on the starting material sieve fractions and at the completion of the testing, the resultant rock was again sieved and remeasured. The bulk surface areas for each

column were determined for the post-leaching rock by taking the individual masses of the sieve fractions specified in the protocol above, multiplying each mass by the surface area (SA), and combining their fractional percent of the total as a weighted linear average.

$$A \times SA_{\text{sieve 1}} + B \times SA_{\text{sieve 2}} + C \times SA_{\text{sieve 3}} = SA_{\text{bulk}} \quad (1)$$

Where: $A + B + C = 1$

A = fraction of total sieve 1 size

B = fraction of total sieve 2 size

C = fraction of total sieve 3 size

Table 1 shows the particle size distributions for the Brush Creek shale and Wadesville sandstone samples used in the 2002 weathering tests and the LRBT coal refuse sample used in the 2003 weathering tests at Lab P. The before-weathering distributions for the shale and sandstone samples are exactly what resulted from crushing the samples; the particle size distribution for the coal refuse sample was reconstructed/adjusted to meet the specification of the revised method as shown in Table 3 in the companion paper (Part 1). The BET measurements of surface area for the shale are an order of magnitude greater than the sandstone and coal refuse surface areas for most size classes (except the 0.149 mm coal refuse pre-weathering). This is probably due to much greater intrinsic porosity in the shale laminae. The sandstone sample was from a very hard and well-cemented lithologic unit, thus there was little difference in the particle size distributions or surface area measurements after weathering. The coal refuse sample showed the greatest change in effective surface area of all samples tested at Lab P in the 2002 and 2003 weathering tests (Table 2). This change is largely due to the reduction in surface area of the two finest size classes (Table 1). Two factors that probably contributed to this reduction are (a) loss of fines during weekly sample collection and (b) weathering of fine-grained pyrite in these size classes.

Table 1. Surface area measurements, sieve analysis, and calculations of effective surface areas, before and after weathering tests.

	Sieve Size	Surface Area (BET) m ² /g		% retained on Sieve		Effective surface area	
		before	after	before	after	before	after
Shale	3/8	15.90	16.40	3.84	4.36	0.611	0.715
	#4	11.10	10.00	21.79	26.83	2.419	2.683
	#8	13.70	11.00	24.13	26.21	3.306	2.883
	#20	14.90	13.80	24.08	22.41	3.588	3.093
	#40	15.70	15.40	9.21	8.23	1.446	1.267
	#100	15.30	15.20	9.76	7.54	1.493	1.146
	#200	15.50	15.40	6.04	2.56	0.936	0.394
	pan	16.90	16.20	1.15	1.87	0.194	0.303
Total						13.993 m²/g	12.484 m²/g
Sandstone	3/8	0.66	0.25	25.50	26.30	0.168	0.066
	#4	0.81	1.00	36.96	35.80	0.299	0.358
	#8	1.42	1.30	14.08	16.60	0.200	0.216
	#20	0.91	0.80	10.77	8.60	0.098	0.069
	#40	1.02	1.41	4.01	4.10	0.041	0.058
	#100	1.75	2.99	4.73	4.70	0.083	0.141
	#200	2.68	4.17	3.24	2.20	0.087	0.092
	pan	2.91	5.00	0.97	1.70	0.028	0.085
Total						1.004 m²/g	1.083 m²/g
Coal Refuse	3/8	0.17	0.40	40.00	37.40	0.068	0.150
	#4	0.92	0.60	25.00	26.90	0.230	0.161
	#8	0.21	0.90	10.00	9.90	0.021	0.089
	#20	0.39	0.50	10.00	8.00	0.039	0.040
	#40	3.39	0.70	5.00	6.40	0.170	0.045
	#100	9.17	1.40	10.00	11.50	0.917	0.161
	#200						
	pan						
Total						1.445 m²/g	0.646 m²/g

Table 2. Summary of change in surface areas after weathering.

Rock Type	Column Size	m ² /g before	m ² /g after	% change
Shale	6"	14.0	12.5	10.71
Shale	6"rpt	14.3	15.1	-5.59
Shale	4"	14.3	14.1	1.40
Shale	2"	14.3	15.5	-8.39
Limestone	6"	3.5	3.0	14.29
Sandstone	6"	1.0	1.1	-10.00
Coal Refuse	6"	1.4	0.6	57.14

Calculation of SA/V ratio

The design of the column experiments allows a direct calculation of the surface area to volume ratio. The surface area for the reconstituted rock mass in the column is calculated as shown above. This quantity is then scaled to the total rock mass in the column. The volume is simply the volume of water drained from the column after each weekly 24-hour fill-and-drain cycle.

$$\frac{SA}{V} = \frac{1000 m SA_{Bulk}}{V} \tag{2}$$

where:

SA/V = surface area to volume ratio (meters⁻¹)

m = mass of solids in column (grams)

SA_{Bulk} = BET surface area of solids (meter-squared/gram)

V = volume of leachate from each drain cycle (liters)

The significance of the surface area to volume ratio in leaching processes is described in Machiels and Pescatore (1983), Pederson et al. (1983), White (1986) and Scheetz et al. (1981).

Leaching Rates and Mechanisms

The theoretical behavior of mineral dissolution and leaching processes is shown in Fig. 2, and described by White (1986), Scheetz et al. (1981), Pedersen et al. (1983), White (1988), and Langmuir (1997). The series of schematic drawings in Fig. 2 are concentration-time relationships for several rate-controlling mechanisms presented by White (1986). Fig. 2a is the schematic dissolution curve for a material (e.g. calcareous shale) that can saturate an aqueous solution, where the dashed line represents the initial slope that would be the observed rate in an experiment providing constantly fresh solvent (e.g. the DI water influent to leaching columns in repeated leaching cycles). Fig. 2b exhibits the parabolic rate law for diffusion-controlled kinetics, while Fig. 2c depicts the linear rate law characteristic of a surface-reaction controlled kinetics truncated by the onset of precipitation. White (1986) states that dissolution “.... may take place by a surface-reaction control mechanism with some contribution from a diffusion control mechanism, the first leading to a linear time dependence and the latter to a parabolic time

dependence.” (p.435). Fig. 2d is the composite curve including overshoot due to supersaturation, the typical case in weathering of pyrite and silicates, followed by a flattening of the slope of the line with increasing time.

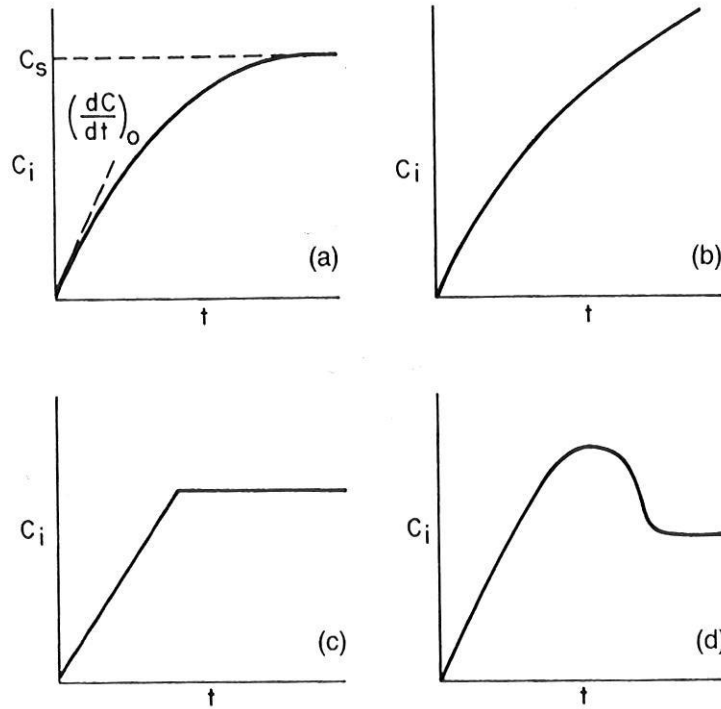


Figure 2. Theoretical behavior of leaching processes (from White, 1986).

Fig. 3 and 4 show concentrations of sulfate and alkalinity through time for the Brush Creek Shale from various leaching columns. Labs M and G used three variations on the leaching method: (a) leaching column, with 24-hour water saturation prior to sampling, with the water having 10% CO_2 air bubbled through it throughout the leaching period; (b) leaching column, with 24-hour water saturation and with water initially saturated with CO_2 ; and (c) humidity cells, with 1-hour saturation of the sample and water initially saturated with CO_2 . All tests were performed on 2-inch columns. Lab P used method (a) only, but the column sizes varied as indicated in Fig. 3. A plot of concentration as a function of the square-root of time could also be used to evaluate the quality of the sample being tested.

Sulfate concentrations from the three diameters of leaching columns at Lab P are plotted in Fig. 3. These plots resemble the leaching behavior shown in Fig. 2d, with the steep initial slope, followed by supersaturation, and then a flattening (6-inch column) or decline (2-inch and 4-inch

columns) in concentration through time for the remainder of the weathering test. Data from Lab M show a similar profile. Notice that these plots do not originate at zero, they extend to negative weeks time, indicating that weathering of the shale samples commenced prior to the start of the leaching column tests (i.e., prior to the initial flush). Representative splits of the same Brush Creek shale samples used in the 2002 weathering tests were used for the 2003 weathering test; these unused splits of shale samples were stored in sealed opaque plastic buckets in a DEP garage for a year, but oxygen was not evacuated from the buckets. Prior to the start of the 2003 tests, the shale samples were rehomogenized and representative splits were retested for total sulfur and neutralization potential, showing no detectable change in percent sulfur and a reduction of 10 to 15 parts per thousand (ppt) NP as compared to the 2002 test results (see sample #32R in Table 1 of the companion paper). The decrease in NP may be due to accumulation of acid salts that neutralized some of the alkalinity produced by the carbonates.

The data for Labs M and P (Fig. 3) show an initial increase in sulfate concentration followed by a decline, with an eventual leveling out of concentration at about 10 weeks. Lab G had a more or less steady output of sulfate. The week-to-week variability at Lab G is also greater than that at the other two labs. The material was more tightly packed in the columns at Lab G than at the other labs. The initial high concentrations at Labs M and P are probably a combination of initial flushing of pyrite oxidation products (despite the efforts at week 0 to flush these products), and higher initial oxidation rates due to greater exposure of pyrite. The lack of similar behavior at Lab G may be related to the greater packing of the material.

Fig. 4 is the time plot of alkalinity concentrations of the Brush Creek shale from leaching columns and humidity cells for the three labs. The plots for Labs M and P resemble the leaching behavior shown in Fig. 2a, or a combination of the initial linear and latter diffusion-controlled mechanisms shown in Fig. 2c and 2b. The time plots in Fig. 4 also depict two noteworthy practical aspects of method performance. First, the highest alkalinity concentrations are produced in the two leaching columns with constant flow of CO₂-enriched air, followed by the two columns with CO₂-saturated influent water, and the two plots with the lowest alkalinity concentrations are the humidity cells. This is less evident at Lab G, because of the widely fluctuating concentrations, but this overall observation still holds true. Second, the dashed lines for Labs M and G represent the duplicate samples. For lab M the duplicates behave very consistently and represent excellent control of the gas-mixture throughout the entire test period.

The wider variation at Lab G probably indicates less precise control of the gas mixture. The widest fluctuations occur in the Lab G humidity cells, followed by the CO₂ saturated water columns. Lab P, which evaluated different diameter columns, had similar alkalinities in the three columns. Fig. 5 is a comparison of calculated P_{CO2} among the three labs for the columns with continuous air flow.

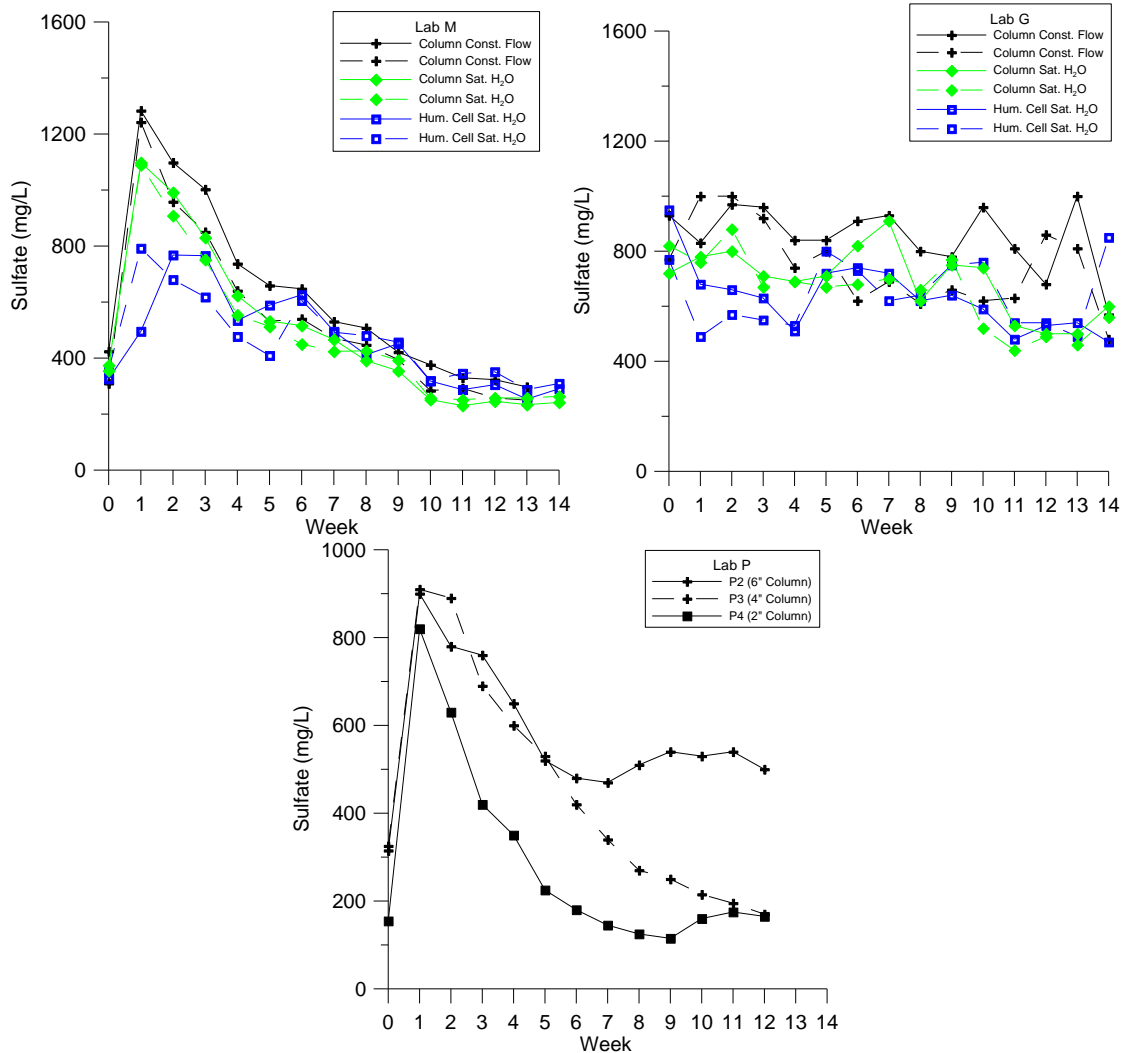


Figure 3. Sulfate concentrations of Brush Creek shale for the three laboratories. Laboratories M and G used three methods: water that had CO₂-enriched water continuously bubbled through the column, with 24 hours of water inundation (black lines); water that was initially saturated with CO₂, and water inundation for 24 hours (green lines); and water initially saturated with CO₂, but water inundation time was one hour (blue lines). For Labs M and P, duplicate samples are shown by the same color. Lab P used the first method only.

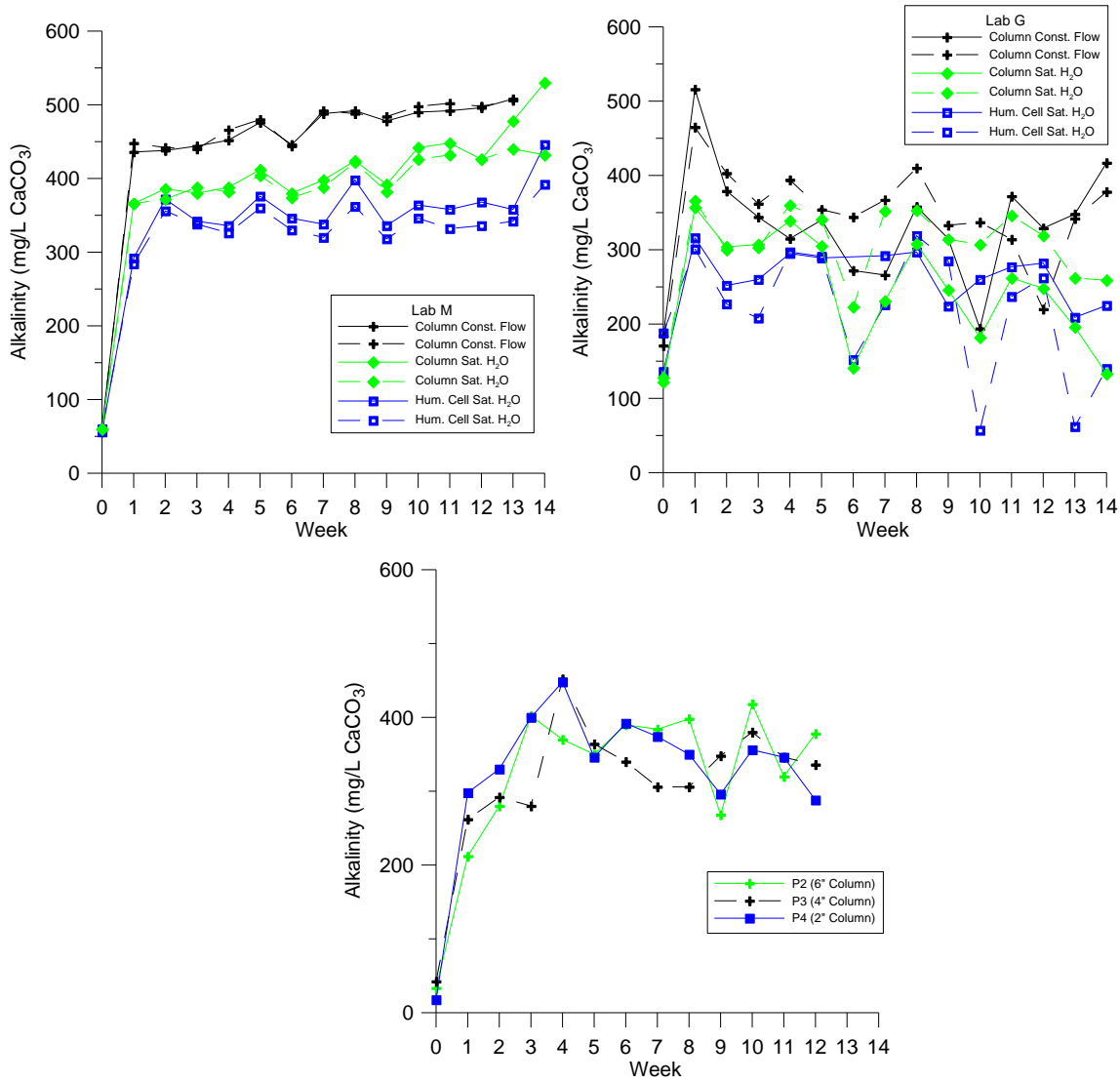


Figure 4. Alkalinity concentrations of Brush Creek shale leaching columns and humidity cells at Labs M, G and P.

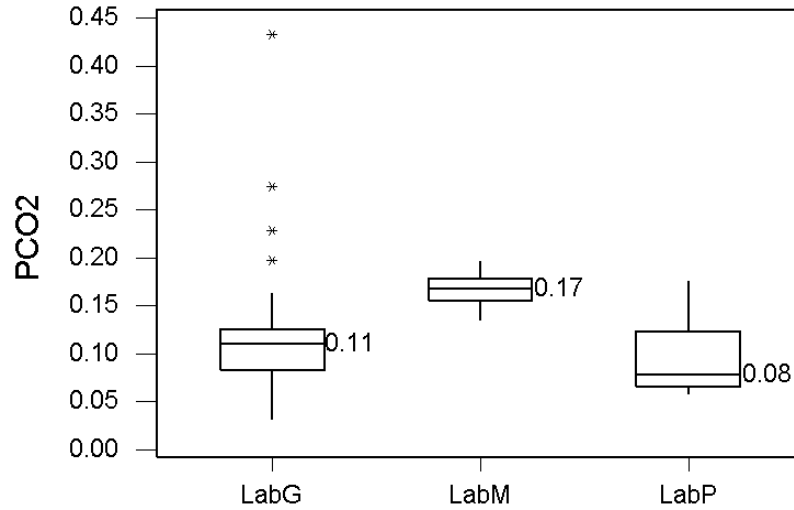


Figure 5. Comparison of P_{CO_2} among laboratories for the leaching columns that had continuous flow of 10% CO_2 -enriched air. Horizontal lines within the “boxes” are medians and the values are plotted next to the box. The “boxes” extend from the 25th to 75 percentile of data and thus encompass the middle 50% of the data. “Whiskers (the vertical lines) show the range of the data to 1.5 times the interquartile range. Asterisks indicated statistical outliers.

Data Processing

Analyses of column effluent produced a very large database concerning many dissolved species and the entire suite of rock types. For purposes of demonstrating the degree to which quantitative rate information can be extracted from the column leach tests, we consider only one rock type, the Brush Creek Shale, and evaluate one dissolved species, sulfur. In other sections of this paper calcite dissolution is also examined. The sulfur in the original rock is shown by the chemical analysis in Table 1 of the companion paper. However, the mineralogical distribution of sulfur is unknown. Prior to the study, the mineralogy of the rock was determined using X-ray diffraction (XRD). Pyrite was present in “trace” (<3%) amounts (Robert Smith, PA Geological Survey, personal communication, 1998), which is consistent with what would be expected with a percent sulfur of 0.9%. Since an unknown amount of rock weathering had taken place in the test samples between the time of collection and the time of the leaching tests, some pyrite had oxidized and probably formed gypsum or other sulfate minerals.

Using the analytical determination of sulfur in the rock analysis and the total mass of rock placed in the columns, it was possible to compute the total sulfur loading (i.e., mass of sulfur,

measured in grams) in the column. The leach solutions were analyzed for sulfate ion, assumed to be the only sulfur-bearing species in solution. Using the volume of water extracted from the columns, it was then possible to calculate the percentage of the initial sulfur loading that had been extracted. Because fresh solutions were used each week, it was necessary to accumulate the percentage of sulfur leached over the weeks of the experiments. The quantity plotted is the total sulfur extracted, expressed as a percentage of the original sulfur loading in the rock. Even at the end of the experiments, only a few percent of the original sulfur had been extracted.

Examination of the data for cumulative sulfur extraction for all columns and all laboratories by a variety of fitting functions showed that log-log (power function) plots with coefficients ranging from 0.42 to 0.499 gave statistically satisfactory fits. These numbers suggest that the theoretical coefficient might be 0.5. Fig. 5 shows a series of plots of the cumulative extracted sulfur as a function of the square root of time. The observed linear fit to the data means that the sulfur fraction, N_s , extracted from the columns can be described by an equation of the form

$$N_s = Kt^{1/2} + F \quad (3)$$

In this equation, K is an empirical rate constant and F is a constant that takes account of the observation that the extracted sulfur does not become zero at time equals zero. The F -term is thus a measure of the “first flush” described above. Values for the coefficients K and F are listed in Table 3. The square root of time dependence in a rate equation usually implies a diffusion controlled mechanism. In the present experiments the oxidation of sulfides at the mineral/water interface, the effect of different particle sizes and surface reactivities, and the transport of dissolved species from the mineral surfaces to the bulk fluid are combined into a single empirical rate expression.

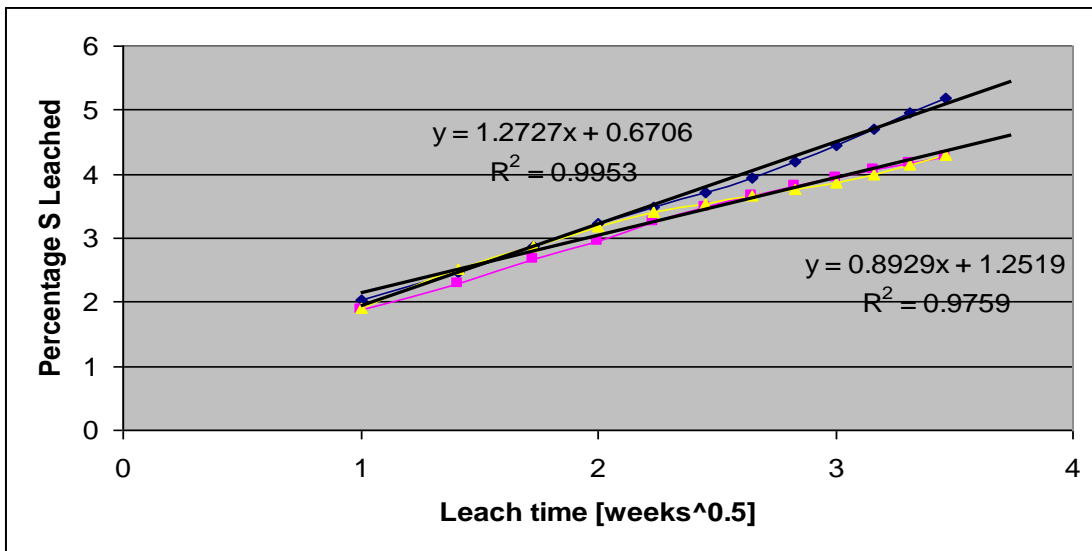
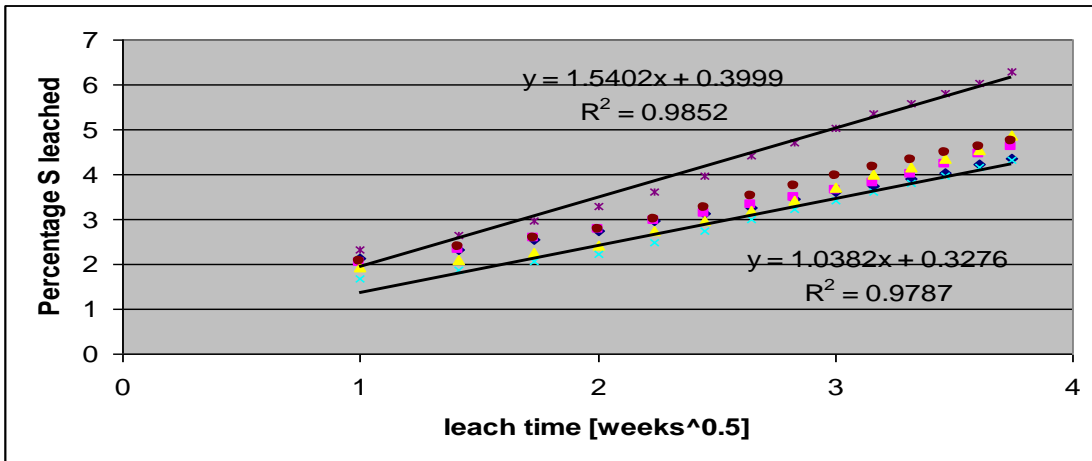
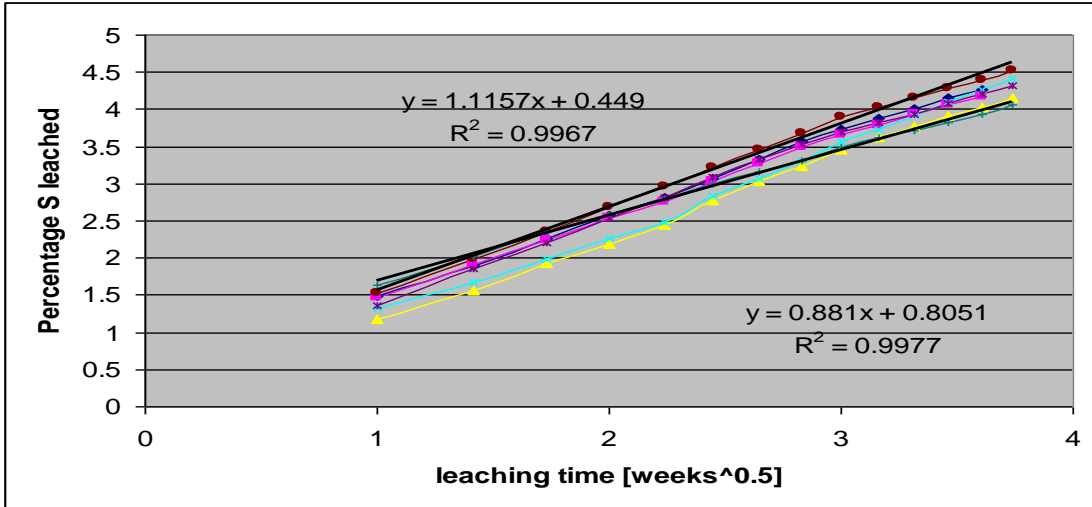


Figure 5. Cumulative % sulfur leached as a function of the square root of time. Top graph is Lab M, middle is Lab G and bottom is Lab P.

Table 3. Fitting Parameters of Sulfur Extraction^a.

Lab ^a	K ^b	F ^c	R ²
Lab M (1)	1.12	0.45	0.997
Lab M (2)	0.88	0.81	0.998
Lab G (1)	1.54	0.40	0.985
Lab G (2)	1.04	0.33	0.979
Lab P (1)	1.27	0.67	0.995
Lab P (2)	0.89	1.25	0.976

^a Data given for maximum (1) and minimum (2) from the collection of data sets.

^b K is in units of (weeks)⁻¹.

^c F is in units of percent extracted and thus dimensionless.

This result suggests that chemical reactions at the surfaces of the grains are fast compared to the movement of dissolved species through the pore spaces between the grains.

Comparison of Cumulative Leaching Rates for Sulfur and Calcite

The following interpretations will deal only with the shale samples. As mentioned earlier, labs M and G analyzed shale in three different ways, (a) columns with CO₂ enriched air bubbled through the water during the period of saturation, (b) humidity cells (columns saturated for only one hour), and (c) columns that were saturated with water that was saturated with CO₂. The cumulative percentage of total sulfur and calcium carbonate depleted per week is plotted in Fig. 6. Power functions were fitted to these data, and they produced higher coefficient of determination (R²) values than exponential or linear functions.

The total amount of CaCO₃ in the columns was determined based on neutralization potential data (ppt CaCO₃). The total amount of CaCO₃ leached per week was calculated as alkalinity, in mg/L CaCO₃, plus alkalinity that was neutralized by sulfide oxidation. For each mole of sulfate produced during pyrite oxidation four moles of H⁺ are produced. This translates to 1.04 mg/L of acidity as CaCO₃ for every mg/L of sulfate. Thus, for example, given a weekly sample with an

alkalinity concentration of 300 mg/L, sulfate of 400 mg/L, and a leachate volume of 300 mL, the total number of grams of CaCO₃ that was dissolved is:

$$\begin{aligned} \text{grams CaCO}_3 &= ((300 \text{ mg/L alk} + (400 \text{ mg/L SO}_4 * 1.04)) * .001) * 0.3 \text{ L} \\ &= 0.215 \text{ grams CaCO}_3 \end{aligned} \quad (4)$$

This type of calculation will not work where there is no excess of alkalinity, that is, under acidic conditions one cannot assume that acids that would be represented by the sulfate ion have been completely neutralized. The amount of CaCO₃ dissolved was not determined from Ca because of the complex nature of the carbonates present in the Brush Creek shale. A comparison between moles of Ca to moles of HCO₃ showed a ratio of less than one, indicating that there were other cations present in the carbonates. XRD analysis identified siderite as well as calcite (R. Smith, PaGS, personal communication 1998). Although dolomite was not detected, some Mg undoubtedly substitutes for Ca and Fe in the carbonate minerals present. A simple adding of Ca + Mg + Fe was not possible because chlorite, a Mg-rich mineral, is a major mineral in the shale and iron is associated with many sources including pyrite. Thus, the use of alkalinity and sulfate as described above.

The total amount of sulfur in each column was calculated using the percent sulfur data using the same method described above for CaCO₃. The amount of sulfur oxidized per week was determined from sulfate. Sulfate is two-thirds oxygen and one-third sulfur by weight. Thus, sulfate divided by three will give mg/L sulfur. As in the equation above, the grams of sulfur were multiplied by the liters of leach water drained from the columns each week.

The total weight of CaCO₃ or S per week was divided by the total mass of CaCO₃ and S available in each column. This normalized the data and gave a percentage of the total mass of CaCO₃ or S per week. These weekly masses (in percent) were added to get a cumulative percent. Table 4 shows the last three weeks of leaching data. Three weeks worth of data is shown because column leaching times varied from 12 to 14 weeks. In all instances, after 12 to 14 weeks, less than 2 percent of the calcium carbonate had weathered, but four to five percent of the sulfur had weathered. The weekly data were then plotted to determine the type of function (equation for a line) that best fit the data. Fig. 7 and 8 are plots of these data. Table 5 provides a

statistical summary of the best fits. For both CaCO_3 and S the linear and power functions fit the data best.

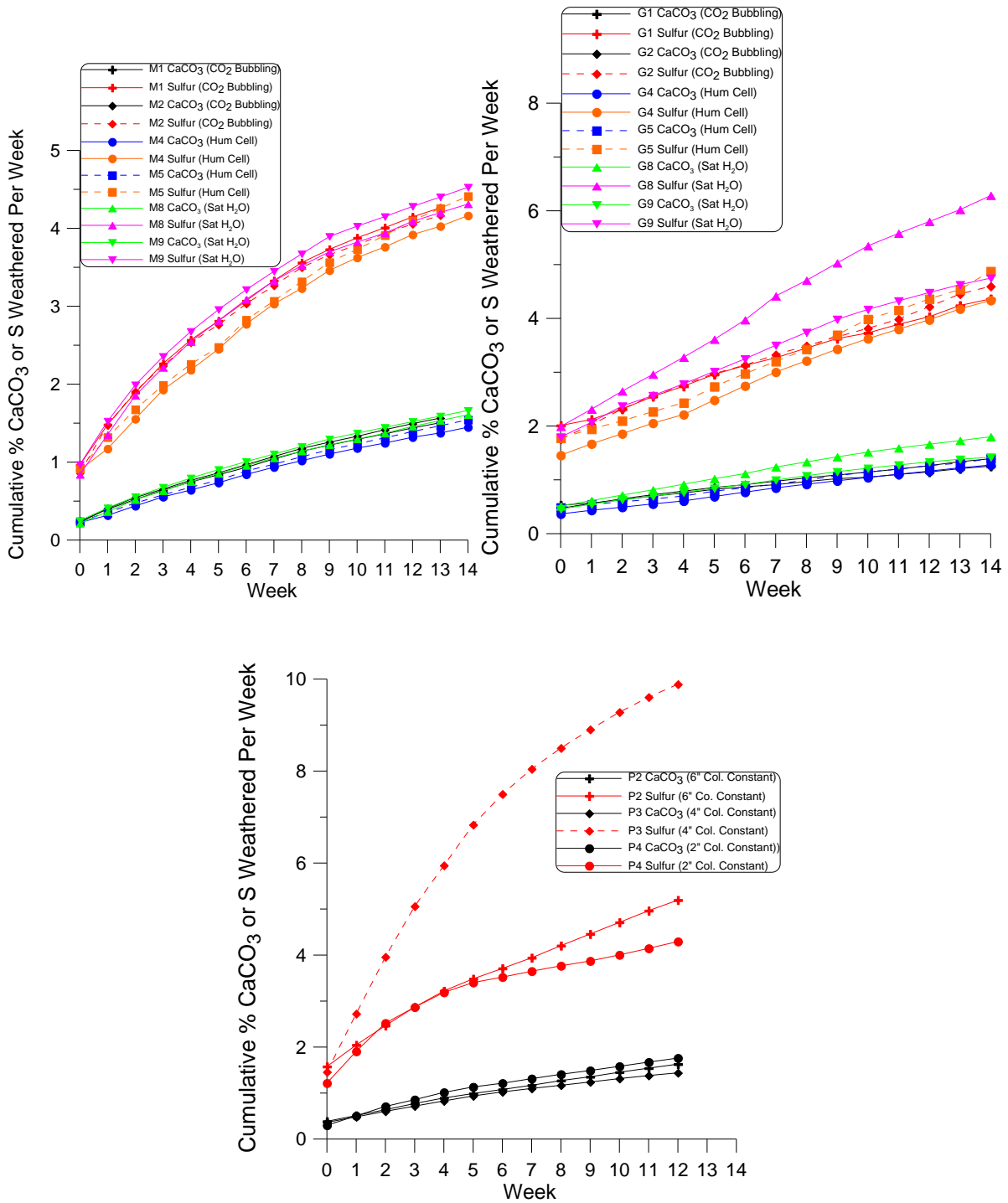


Figure 6. Cumulative percent sulfur and CaCO_3 leaching rates per week for all columns and humidity cells at Labs M, G, and P.

Table 4. Total percent of calcite and sulfur weathered for each cell at end of test. Leaching times varied between 12 and 14 weeks for the columns.

Column	CaCO ₃ : Week			S: Week		
	12	13	14	12	13	14
M1	1.44	1.51		4.14	4.26	
M2	1.49	1.57		4.05	4.17	
M4	1.32	1.37	1.45	3.91	4.03	4.16
M5	1.39	1.47	1.54	4.10	4.26	4.41
M8	1.46	1.53	1.61	4.09	4.20	4.31
M9	1.52	1.59	1.66	4.28	4.40	4.53
MX	1.70	1.80	1.90	3.82	3.94	4.07
GC1	1.15	1.21	1.26	4.03	4.24	4.36
GC2	1.26	1.34	1.39	4.22	4.45	4.60
GC4	1.16	1.22	1.28	3.97	4.18	4.34
GC5	1.27	1.31	1.40	4.36	4.54	4.88
GC8	1.66	1.73	1.80	5.80	6.02	6.28
GC9	1.33	1.38	1.42	4.48	4.63	4.75
PSU2	1.63			5.22		
PSU3	1.44			4.27		
PSU4	1.76			4.29		

Table 5. R² values and power exponents for leaching columns.

Column	CaCO ₃				Sulfur			
	Linear R ²	Exponential R ²	Power R ²	Power Exponent	Linear R ²	Exponential R ²	Power R ²	Power Exponent
M1	0.989	0.884	0.993	0.540	0.958	0.847	0.998	0.427
M2	0.988	0.866	0.992	0.542	0.950	0.819	0.998	0.417
M4	0.992	0.897	0.996	0.594	0.972	0.881	0.997	0.500
M5	0.995	0.902	0.991	0.578	0.984	0.895	0.991	0.480
M8	0.987	0.859	0.998	0.570	0.940	0.806	0.998	0.444
M9	0.985	0.868	0.996	0.545	0.947	0.824	0.999	0.423
MX	0.994	0.898	0.990	0.537	0.945	0.843	0.999	0.350
G1	0.996	0.971	0.966	0.311	0.996	0.973	0.965	0.287
G2	0.996	0.955	0.971	0.354	0.994	0.958	0.968	0.316
G4	0.998	0.968	0.955	0.445	0.997	0.972	0.950	0.395
G5	0.997	0.984	0.934	0.388	0.996	0.989	0.925	0.376
G8	0.995	0.952	0.972	0.439	0.995	0.960	0.965	0.411
G9	0.995	0.957	0.964	0.391	0.992	0.957	0.965	0.339
P2	0.994	0.927	0.989	0.477	0.985	0.918	0.989	0.380
P3	0.985	0.911	0.993	0.456	0.942	0.865	0.997	0.342
P4	0.972	0.841	0.999	0.499	0.880	0.753	0.989	0.310

Red is highest R²

Blue is 2nd highest R²

Power Exponent: Red is >0.4 and <0.6

Predictive Capabilities

The fitting of a function through the data allows prediction of results into the future. Fig 7 shows power function best-fit lines extended to six years. The leaching results are plotted to show how closely the data fit the projected line. The results suggest that if the sample were to be leached for 6 years the rate of pyrite oxidation would continue to be greater than that of carbonate dissolution. Considering the fact that the water remained alkaline throughout the test period, which had the highest rates of pyrite oxidation (steepest part of curve), this sample can be expected to produce alkaline drainage long into the future. In fact, the pyrite should be exhausted prior to calcite exhaustion. Presuming that the rates do not change, at the end of six years 16 to 20% of the pyrite would be consumed, whereas only 6 to 8% of the carbonate would be consumed.

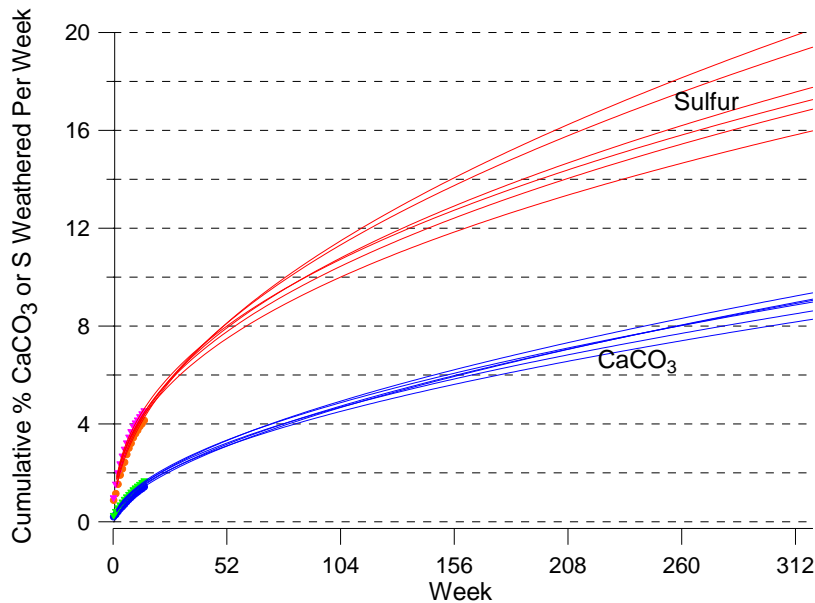


Figure 7. Power function best-fit lines for the cumulative percent CaCO₃ and S data for Lab M. Rates are predicted to 6 years.

Example best-fit equations are presented in equations (5) and (6). These are for results from Lab M, Column 9 (water saturated with CO₂).

$$\ln(\text{Cum. CaCO}_3) = 0.545 \times \ln(\text{weeks}) - 0.950 \tag{5}$$

and

$$\ln(\text{Cum. S}) = 0.423 \times \ln(\text{weeks}) + 0.407 \tag{6}$$

Solubility Controls on Weathering

The data were also evaluated to determine whether calcite or gypsum were at saturation. The columns that had CO₂ enriched air bubbled through them during the period of water saturation were typically at saturation with calcite. By contrast, the humidity cells were often undersaturated with respect to calcite. The columns that used CO₂ water during the water saturation period were generally at or above saturation with calcite. The columns of Lab G had lower saturation indices for this later group than did Lab M. Only a handful of samples were ever near or at saturation with respect to gypsum, and this only in the columns and never in the humidity cells. Saturation or near saturation with gypsum also only occurred during the early weeks when pyrite oxidation and sulfate weathering products dissolution rates were the greatest. The saturation indices are provided in Appendix A at the end of this paper.

Saturation indices for calcite (Appendix A) give an indication as to whether or not the water in the column reached saturation with respect to calcite. The oversaturation in most instances is an artifact of CO₂ degassing during sample collection (see Hornberger et al., 2003 for detailed explanation). With the exception of Humidity Cell results for Lab G, most column waters were near or at saturation with calcite. As discussed earlier, calcite dissolution is not limited to just the solubility of calcite. Calcite also dissolves in response to acid generated by pyrite oxidation. Thus, the total amount of calcite dissolved is a function of calcite dissolved to neutralize acid plus calcite that dissolves in solution up to the point of saturation.

The water is almost always undersaturated with respect to gypsum throughout the tests at both Labs G and M (Appendix A). The only exceptions were early in some of the leaching tests, where in some instances during weeks one through three gypsum was at or near saturation. Saturation during the early weeks may be due to the initial high pyrite oxidation rates combined with continued flushing of accumulated pyrite weathering products. After this initial period, however, gypsum was always undersaturated. Undersaturation of gypsum provides confidence that sulfate is in fact conservative and can be used as a proxy for pyrite oxidation rates.

Gas Composition

The goal of this study was to leach calcareous rocks at Pco₂ concentrations similar to those seen on mine sites. The target Pco₂ was 10%. To test whether or not the rocks were weathering at this target concentration, Pco₂ was calculated based on pH, alkalinity, calcium concentration

and temperature. Calcium and alkalinity were assumed to be conservative. Equilibrium computations were performed on a spreadsheet developed by C.A. Cravotta III (USGS, personal communication; see Hornberger et al., 2003 for details on the method). Table 6 shows the calculated P_{CO_2} for the different types of leaching columns for Lab G and Lab M. The reason that some columns exceeded 10% CO_2 is that the shale produced CO_2 as a result of acid from pyrite oxidation products reacting with the carbonate minerals. The following equation expresses this process:



The columns were generally at or greater than 10% CO_2 , with the continuous flow columns having the highest values. The humidity cells were consistently less than 10% CO_2 .

Table 6. Calculated average (mean) percent CO_2 in columns and humidity cells for shale at Labs M and G.

	Lab M	Lab G
001 Column Continuous CO_2 Flow	16.8	13.6
002 Column Continuous CO_2 Flow	16.5	13.4
004 Humidity Cell CO_2 Saturated H_2O	8.4	7.4
005 Humidity Cell CO_2 Saturated H_2O	7.5	7.3
008 Column CO_2 Saturated H_2O	11.9	10.2
009 Column CO_2 Saturated H_2O	10.6	7.5

Comparison of Leaching Data to the Real World

The leaching test is being developed as a mine drainage prediction tool. For any predictive method to be useful it must be able to predict field conditions. Table 7 compares representative laboratory leaching results with field data from sites that have the same material present. The field samples for the Brush Creek shale are from a 16-acre (6.5 ha) surface mine in Westmoreland County, Pennsylvania that is mining the Brush Creek coal. The overburden of the Brush Creek coal is the Brush Creek marine zone, which includes the Brush Creek shale. The mine is about 14 miles (24 km) from where the Brush Creek shale sample was collected. The field samples for the refuse are from the Leachburg refuse pile in Armstrong County, Pennsylvania. The Leachburg refuse pile is composed of Lower Kittanning refuse and is located

only a couple of miles (kms) from where the refuse in this study was obtained. Many factors combine to make the laboratory and field samples behave differently. For example, the Leachburg refuse pile has been weathering in the same location for many decades. Table 1 in the companion to this paper (Part 1) shows sulfur concentrations for the Leachburg refuse pile. Sulfur is typically 2.5 to 3%, whereas in the fresh refuse used for this study the sulfur is 6.6 to 7.7%. The lower sulfur in the Leachburg refuse is probably due to weathering losses and less efficient mining and coal preparation decades ago (i.e., more dilution with low sulfur rock), as compared to today. The Brush Creek mine would disturb more rocks than just the Brush Creek shale. Even with these limitations, the leaching data is typically a factor of two or less compared to the field data.

Table 7. Comparisons between laboratory leaching data and field data for the Brush Creek shale and the Lower Kittanning coal refuse. The example laboratory samples are representative of the laboratory results. Field data for the Lower Kittanning refuse are from Hornberger and Brady (1998, Table 7.1) and the Brush Creek data are from M. Gardner (personal communication, 2004). Units are mg/L, except for pH, which is in standard units.

Rock Type	Lab or Field	pH	Alk	Acidity	SO ₄	Fe	Mn	Al
Brush Creek Shale	Lab M Wk 13 Const. Flow	6.8	508	0	297	0.01	0.40	0.01
Brush Creek Shale	Lab G Wk 4 Const. Flow	6.6	339	0	690	0.07	1.63	<0.1
Brush Creek Mine	Field	6.6	162	0	586	0.30	1.18	<0.5
Brush Creek Mine	Field	6.4	200	0	789	0.35	3.65	<0.5
LK Refuse	Lab M Wk 11	1.3	0	28000	28059	7771	18	124
LK Refuse	Lab P Wk 8	1.9	0	26062	24516	9480	10.9	105
LK Refuse	Field	2.4	0	16594	11454	>300	16.5	>500
LK Refuse	Field	2.0	0	10383	14565	2200	3.3	

Conclusions

The following observations are made:

1. The surface area of the Brush Creek shale was an order of magnitude greater than that for the sandstone and coal refuse, showing that the surface areas of different types of rocks can be quite different.
2. The surface area after weathering was essentially the same for the sandstone, just slightly less for the shale and limestone, and about half for the refuse. The sandstone is strongly cemented and probably underwent little weathering. Due to the high pyrite content the refuse underwent the most weathering and had the greatest decrease in surface area. Both the limestone and the shale showed some decrease in surface area.
3. Sulfur weathering appeared to follow diffusion-controlled kinetics. Carbonate weathering was controlled by reaction with acid from pyrite oxidation products (neutralizing acid) and was limited by calcite saturation.
4. The goal of 10% CO₂ for the shale sample was achieved in the two types of columns, but not in the humidity cell.
5. After 12 to 14 weeks of leaching, less than 2 percent of the calcite had weathered from the shale, compared to 4 or 5 percent of the pyrite. Thus, the pyrite is weathering faster than the calcite and predictions show that this rock would continue to produce alkaline water for years.
6. Field data for the same stratigraphic units compare within a factor of two to that of the leaching results.

Acknowledgements

The authors thank Gwendelyn Geidel and Charles Bucknam for their helpful reviews of this paper.

Literature Cited

- Brantley, S.L. and N.P. Mellott. 2000. Surface area and porosity of primary silicate minerals. American Mineralogist, Vol. 85, pp. 1767-1783. <http://dx.doi.org/10.2138/am-2000-11-1220>.
- Brunauer, S., P.H. Emmett and E. Teller, (1938). J. Amer. Chem. Soc. Vol. 60, p. 309.
- Buckwalter, C.Q., L.R. Pederson and G. L. McVay J. 1982. Non-Crystalline Solids, Vol. 49,

p. 397 [http://dx.doi.org/10.1016/0022-3093\(82\)90135-1](http://dx.doi.org/10.1016/0022-3093(82)90135-1)

Cravotta, C.A., III, D.L. Dugas, K.B.C. Brady and T.E. Kovalchuk. 1994. Effects of selective handling of pyritic, acid-forming materials on the chemistry of pore gas and ground water at a reclaimed surface coal mine, Clarion County, PA, USA. U.S. Bureau of Mines Special Publication SP 06A-94, p. 365-374.

Ethridge, E.C., D.E. Clark and L.L. Hench. 1979. J. Phys. Chem. Glasses Vol 25, No. 2, p. 35.

Hammack, R.W. and G.R. Watzlaf. 1990. The effect of oxygen on pyrite oxidation. In: Proceedings of the 1990 Mining and Reclamation Conf. and Exhibition, Vol. 1, Morgantown: West Virginia University, p. 257-264.

<https://doi.org/10.21000/JASMR90010257>

Hench, L.L., D.E. Clark and E.L. Yen-Bower, 1980. Nuclear and Chemical Waste Management 1, 59. [http://dx.doi.org/10.1016/0191-815X\(80\)90029-7](http://dx.doi.org/10.1016/0191-815X(80)90029-7)

Hornberger, R.J. and K.B.C. Brady. 1998. Kinetic (leaching) tests for the prediction of mine drainage quality. In: Coal Mine Drainage Prediction and Pollution Prevention in Pennsylvania, Harrisburg: Pennsylvania Department of Environmental Protection, pp. 7-1 to 7 – 54.

Hornberger, R.J., K.B.C. Brady, J.E. Cuddeback, W.A. Telliard, S.C. Parsons, B.E. Scheetz and T.W. Bergstresser. 2003. Development of the ADTI-WP1 (humidity cell) and ADTI-WP2 (leaching column) standard weathering procedures for coal mine drainage prediction. In: Proceedings 2003 SME Annual Meeting, preprint 03-069. Littleton, CO. Society for Mining, Metallurgy and Exploration.

Hornberger, R.J., K.B.C. Brady, W.B. White, B.E. Scheetz, J.E. Cuddeback, W.A. Telliard, S.C. Parsons, C.M. Loop, T.W. Bergstresser, C.R. McCracken, Jr., and D. Wood, 2004. Refinement of ADTI-WP2 Standard Weathering Procedures and Evaluation of Particle Size and Surface Area Effects upon Leaching Rates. Part 1. In: National Meeting American Society of Mining and Reclamation and the 25th West Virginia Surface Mine Drainage Task Force, April 18-24, 2004. Published by ASMR, Lexington, KY.

<https://doi.org/10.21000/JASMR04010916>

Langmuir, D. 1997. Aqueous Environmental Geochemistry. New Jersey, Prentice-Hall, 600 p.

Lusardi, P.J. and P.M. Erickson. 1985. Assessment and reclamation of an abandoned acid-producing strip mine in northern Clarion County, Pennsylvania. In 1995 Symposium on Surface Mining Hydrology, Sedimentology and Reclamation (Univ. KY, Lexington, KY), p. 313-321.

- Machiels, A.J. and C. Pescatore. 1983. The Functional Dependence of Leaching on the Surface Area-to-Solution Volume Ratio. *Mater. Res. Soc. Symp. Proc.*, 15, 209-16. <http://dx.doi.org/10.1557/PROC-15-209>.
- Oversby, V.M. 1982. PNL-4382, Pacific Northwest Laboratory, Richland, Washington 99352, 97 p.
- Pederson, L.R., C.Q. Buckwalter, G.L. McVay and B.L. Riddle. 1983. Glass surface area to solution volume ratio and its implications to accelerated leach testing. In: *Materials Research Society Symposium Proceedings*, Vol. 15. New York: Elsevier Science Publishing Co. pp. 47-54.
- Scheetz, B.E., W.P. Freeborn, S. Komarneni, S.D. Atkinson and W.B. White. 1981. Comparative study of hydrothermal stability experiments: Application to Simulated Nuclear Waste Forms. *Nuclear and Chemical Waste Management*, Vol. 2, pp. 229 – 236. [http://dx.doi.org/10.1016/0191-815X\(81\)90020-6](http://dx.doi.org/10.1016/0191-815X(81)90020-6)
- White, W.B. 1986. Dissolution mechanisms of nuclear waste glasses: A critical review. In: *Advances in Ceramics*, Vol. 20 Nuclear Waste Management II, the American Ceramic Society, pp. 431 – 442.
- White, W.B. 1988. *Geomorphology and Hydrology of Karst Terrains*. Oxford University Press, Inc., 464 p.
- Yates, D.J.C. 1992. Physical and chemical adsorption – measurement of solid surface areas. In: *Encyclopedia of Materials Characterization: Surfaces, Interfaces, Thin films*. Edited by C.R. Brundle, C.A. Evans, Jr. and S. Wilson, Boston MA: Butterworth-Heinemann, pp. 736-744. <http://dx.doi.org/10.1016/B978-0-08-052360-6.50069-2>.

Appendix A

Saturation indices for calcite and gypsum for all weeks of testing at Labs G and M. Numbers in **bold** indicate the water was at or near saturation. The first column, named “column” identified the specific leaching column or humidity cell and the leaching method. Sh or SH identifies the sample as shale, Col identifies the leaching procedure as “column leaching”; HC identifies the method as “humidity cell,” CF indicates constant flow of CO₂-enriched air, S indicates water saturated with CO₂. Thus, 002Sh ColCF indicates that this is a shale sample that was in leaching column 2 and that had continuous flow of CO₂-enriched air, and 004SH HC S indicates that this was column 4, which was a humidity cell and it had CO₂-saturated water.

Column	Week	Lab G		Lab M	
		SI cal	SI gyp	SI cal	SI gyp
001Sh ColCF	0	0.450	-0.152	0.056	-0.781
001Sh ColCF	1	-0.042	-0.110	0.288	0.016
001Sh ColCF	2	0.563	-0.137	0.308	-0.029
001Sh ColCF	3	0.411	-0.062	0.422	-0.061
001Sh ColCF	4	0.177	-0.048	0.170	-0.242
001Sh ColCF	5	0.296	-0.233	0.301	-0.282
001Sh ColCF	6	0.317	-0.182	0.172	-0.376
001Sh ColCF	7	0.633	-0.143	0.340	-0.454
001Sh ColCF	8	0.236	-0.231	0.017	-0.452
001Sh ColCF	9	0.159	-0.268	0.296	-0.520
001Sh ColCF	10	-0.018	-0.158	0.153	-0.584
001Sh ColCF	11	-0.008	-0.192	0.263	-0.712
001Sh ColCF	12	-0.265	-0.462	0.056	-0.713
001Sh ColCF	13	0.027	-0.133	0.277	-0.743
001Sh ColCF	14	-0.520	-0.389		
002Sh ColCF	0	0.562	-0.280	-0.006	-1.001
002Sh ColCF	1	0.081	-0.007	0.281	-0.005
002Sh ColCF	2	0.423	-0.094	0.465	-0.130
002Sh ColCF	3	0.428	-0.085	0.333	-0.190
002Sh ColCF	4	0.145	-0.303	0.277	-0.339
002Sh ColCF	5	0.217	-0.247	0.274	-0.418
002Sh ColCF	6	0.332	-0.418	0.162	-0.466
002Sh ColCF	7	0.528	-0.308	0.315	-0.503
002Sh ColCF	8	0.156	-0.380	0.084	-0.526
002Sh ColCF	9	0.268	-0.341	0.341	-0.497
002Sh ColCF	10	0.061	-0.379	0.097	-0.777
002Sh ColCF	11	-0.363	-0.365	0.223	-0.752
002Sh ColCF	12	-0.487	-0.211	0.161	-0.855
002Sh ColCF	13	-0.025	-0.160	0.266	-0.806
002Sh ColCF	14	-0.322	-0.516		
004SH HC S	0	0.318	-0.143	-0.091	-0.970
004SH HC S	1	-0.616	-0.274	-0.011	-0.568
004SH HC S	2	0.220	-0.358	0.179	-0.212
004SH HC S	3	-0.167	-0.370	-0.013	-0.256
004SH HC S	4	0.269	-0.484	0.095	-0.446
004SH HC S	5	0.053	-0.248	0.176	-0.421
004SH HC S	6		-0.272	0.189	-0.332
004SH HC S	7	0.091	-0.323	-0.194	-0.611
004SH HC S	8	-0.022	-0.401	0.044	-0.610
004SH HC S	9	-0.126	-0.373	0.106	-0.543
004SH HC S	10	0.102	-0.433	0.002	-0.714
004SH HC S	11	-0.018	-0.567	0.009	-0.810
004SH HC S	12	-0.056	-0.471	0.066	-0.780
004SH HC S	13	-0.231	-0.507	0.032	-0.852
004SH HC S	14	0.001	-0.556	-0.074	-0.777

005SH HC S	0	0.522	-0.263	-0.022	-0.902
005SH HC S	1	-0.648	-0.518	-0.002	-0.238
005SH HC S	2	0.116	-0.468	0.092	-0.320
005SH HC S	3	-0.229	-0.484	0.037	-0.371
005SH HC S	4	0.144	-0.498	0.011	-0.513
005SH HC S	5	0.065	-0.205	0.127	-0.636
005SH HC S	6	-0.113	-0.336	0.099	-0.422
005SH HC S	7	-0.139	-0.399	-0.165	-0.575
005SH HC S	8	-0.159	-0.358	0.013	-0.516
005SH HC S	9	-0.271	-0.264	0.071	-0.537
005SH HC S	10	-1.758	-0.330	-0.030	-0.756
005SH HC S	11	-0.255	-0.489	-0.050	-0.693
005SH HC S	12	-0.192	-0.468	-0.028	-0.701
005SH HC S	13	-0.245	-0.617	-0.046	-0.802
005SH HC S	14	-0.254	-0.175	-0.108	-0.750
008Sh CoIS	0	0.595	-0.320	-0.121	-0.880
008Sh CoIS	1	-0.407	-0.161	0.279	-0.076
008Sh CoIS	2	0.461	-0.210	0.220	-0.107
008Sh CoIS	3	0.270	-0.266	0.293	-0.190
008Sh CoIS	4	-0.026	-0.331	0.292	-0.359
008Sh CoIS	5	-0.174	-0.313	0.300	-0.419
008Sh CoIS	6	-0.597	-0.240	0.170	-0.501
008Sh CoIS	7	-0.203	-0.120	0.363	-0.509
008Sh CoIS	8	-0.154	-0.348	0.100	-0.606
008Sh CoIS	9	-0.333	-0.254	0.300	-0.607
008Sh CoIS	10	-0.583	-0.278	0.099	-0.845
008Sh CoIS	11	-2.180	-0.463	0.182	-0.916
008Sh CoIS	12	-0.450	-0.629	0.068	-0.872
008Sh CoIS	13	-0.240	-0.504	0.267	-0.826
008Sh CoIS	14	-1.105	-0.439	0.062	-0.909
009Sh CoIS	0	0.548	-0.241	-0.037	-0.912
009Sh CoIS	1	-0.124	-0.212	0.272	-0.092
009Sh CoIS	2	0.390	-0.134	0.117	-0.144
009Sh CoIS	3	0.149	-0.308	0.240	-0.270
009Sh CoIS	4	0.088	-0.346	0.228	-0.434
009Sh CoIS	5	0.129	-0.389	0.253	-0.435
009Sh CoIS	6	0.237	-0.382	0.029	-0.573
009Sh CoIS	7	0.405	-0.304	0.266	-0.598
009Sh CoIS	8	0.181	-0.353	0.120	-0.547
009Sh CoIS	9	-0.009	-0.233	0.271	-0.557
009Sh CoIS	10	-0.026	-0.491	0.110	-0.828
009Sh CoIS	11	0.016	-0.568	0.151	-0.858
009Sh CoIS	12	-0.074	-0.674	0.164	-0.845
009Sh CoIS	13	0.191	-0.538	0.205	-0.806
009Sh CoIS	14	-0.066	-0.420	0.070	-0.875